Acta Scientific Clinical Case Reports

Volume 3 Issue 4 April 2022

Review Article

Some Results Related to the Application of the ESPVR to the Study of Cardiac Mechanics

Rachad Mounir Shoucri*

Department of Mathematics and Computer Science, Royal Military College of Canada, Kingston, Canada

***Corresponding Author:** Rachad Mounir Shoucri, Department of Mathematics and Computer Science, Royal Military College of Canada, Kingston, Canada.

Received: February 14, 2022

Published: March 31, 2022

© All rights are reserved by **Rachad Mounir Shoucri.**

Abstract

Relations previously derived between the ejection fraction (EF) and the parameters describing the linear model of the end-systolic pressure-volume relation (ESPVR) of the left-ventricle of the heart have been used to derive indexes that can be used to study the mechanics of cardiac contraction and some aspects of heart failure (HF). The present study presents further applications of these indexes to clinical data published in the medical literature in a way to show the consistency of the mathematical formalism used. An important aspect of this mathematical formalism is the introduction of the peak active pressure generated by the myocardium during an ejecting contraction (also called isovolumic pressure P_{isom} by physiologists) in the mathematical formalism describing the ESPVR. The link between the change of volume of the left-ventricle and the pressures acting on the myocardium is given by two parameters, the slope E_{max} of the ESPVR, and the intercept V_{om} of the ESPVR with the horizontal volume-axis. It is observed that no one index gives perfect segregation between all clinical groups, some indexes are better than others depending on the clinical groups considered. It is also observed that bivariate (or multivariate) analysis of data gives better classification of clinical data than univariate analysis (like using only EF).

Keywords: Ejection Fraction; ESPVR; Heart Failure

Introduction

Early study of the pressure-volume relation (PVR) in the heart left ventricle goes back to the work of Frank in the nineteenth century [1], a review of this work has been published by Kuhtz-Buschbeck., *et al*. [2]. When the cardiac muscle reaches its maximum state of activation near end-systole, the left ventricular pressure is indicated by P_m, and the left ventricular volume by V_m. As in previous studies by the author, we take $P_m \approx P_{es}$ the end-systolic pressure, and $V_m \approx V_{es}$ the end-systolic volume (end-systole is defined as the minimum value of the left ventricular volume V at which the time derivative $dV/dt = 0$). With this notation the ejection fraction (EF) is calculated as $EF \approx (V_{ed} - V_m)/V_{ed}$ (the end-diastolic value V_{ed} is defined as the maximum value of the left ventricular volume V at which the time derivative $dV/dt = 0$). When the cardiac muscle (myocardium) reaches its maximum state of activation near end-systole, the position of the point (P_m, V_m) on the PV- loop varies along a tangential non-linear curve called the end-systolic pressure-volume relation (ESPVR). Properties of the non-linear ESPVR and its linear approximation have been reviewed in several articles [1-7]. In the present study, the ESPVR is approximated by the straight line d_3V_{om} shown in figure 1. (Note that we use the same symbol V_{om} to indicate the point of interception of the line d_3V_{om} with the volume axis in figure 1, as well as the value of the corresponding volume used in the calculation).

An important feature of the mathematical formalism used in this publication and in previous publications by the author in order to study the PVR was the introduction of the active pressure generated by the myocardium (also called isovolumic pressure

P_{iso} by physiologists) in the mathematical formalism describing the PVR [8-10]. Its maximum value P_{isom} is shown in figure 1, the introduction of which has indicated some new aspects of the relation between the ESPVR represented by line d_3V_{om} and the areas of the triangle $d_3V_{om}V_{ed}$ under the ESPVR as discussed in previous studies [11-17]. In particular figure 5 and figure 10 show how different pathologies of the left ventricle with different areas under the ESPVR can have the same EF as a normal left ventricle.

The problem of the heart failure (HF) with normal ejection fraction (EF) (abbreviated HFnEF), HF with reduced EF (HFrEF), or HF with preserved EF (HFpEF) has been studied by various researchers by using various approaches [18-24]. An important application of the ESPVR introduced by the author in [25] and discussed in this study is the possibility to classify the state of the left ventricle into normal, mildly depressed or severely depressed state. It should be clear that the problem of HF is a complex problem that is influenced by ejection and loading condition, left ventricular filling, the intrinsic state and the metabolism of the myocardium. We are looking at the problem of HF from one angle by looking at indexes derived from the mechanics of cardiac contraction.

In successive sections of this study concepts and mathematical formalism are first explained, then applications to clinical data published in the literature are presented that show the consistency of the mathematical formalism used. Although the discussion is limited to the left ventricle, the extension of the ideas presented in this study to the right ventricle is possible [26-28].

This study is a development related to a communication by the author under the title : Indexes derived from the end systolic pressure volume applied to the study of heart failure, presented to the "3rd Euro-Global Experts Meeting on Medical Case Reports", June 30 - July 02, 2016, Valencia, Spain, link at: https://www.omicsonline.org/2165-7920/Euro-Case-Reports-2016_Keynote.digital/files/assets/common/downloads/Euro-Case-Reports-2016_Keynote.pdf

PVR and ESPVR

The cylindrical model of the left ventricle has been explained in previous publications [8-17] and it will not be repeated here. We concentrate directly on figure 1 that represents in a simplified way the PVR in the left ventricle. During a normal ejecting contraction the left ventricular pressure P_m is assumed constant, and the PV-loop is represented by the rectangle $V_{ed}d_2d_1V_m$. During a normal ejecting contraction, the equilibrium of pressures at the surface of the endocardium is given by

$$P_{iso} - P = E (V_{ed} - V) \text{ ---(1)}$$

Which can be split in two equations

$$P_{iso} = E (V_{ed} - V_o) \text{ --------(2)}$$

$$P = E (V - V_o) \text{ -------(3)}$$

Near end-systole when the myocardium reaches its maximum state of activation, the ESPVR is represented in figure 1 by the tangential line d_3V_{om} described by the equation

$$P_{isom} - P_m = E_{max} (V_{ed} - V_m) \text{ ----------(4)}$$

Which can be split in two equations

$$P_{isom} = E_{max} (V_{ed} - V_{om}) \text{ -----(5)}$$

$$P_m = E_{max} (V_m - V_{om}) \text{---------- (6)}$$

As previously mentioned, we have assumed for simplicity that $P \approx P_m$ is constant during the ejection phase as shown in figure 1. Note from Equ. 4 how the stroke volume $SV \approx (V_{ed} - V_m)$ is related to the pressure gradient $P_{isom} - P_m$, P_{isom} is determined during the diastolic phase by the intrinsic state of the myocardium and the initial stretch of the cardiac muscle V_{ed} according to the Frank-Starling mechanism. Equs 1 and 4 can be looked at in two ways:

- If P_{iso} (or P_{isom}) is kept constant and P and V are varied, one gets a line of slope E (or Emax) as if a balloon is inflated against a constant pressure P_{iso} (or P_{isom}).
- If P_{iso} is allowed to vary with P and V, one gets the closed PV-loop of a normal ejecting contraction represented in a simplified way by the rectangle $V_{ed}d_2d_1V_m$. In this case the point (P_{iso}, V) will move near the line d_2d_4 in figure 1 during the contraction phase to reach the maximum value P_{isom} determined by the initial stretch of the muscle V_{ed} according to the Frank-Starling mechanism.

Figure 1 shows the variation ΔP_{iso} and ΔP_{isom} corresponding to the variation ΔV_{ed} in the intial stretch of the cardiac muscle at end-diastole according to the Frank-Starling. The area $V_{ed}\ d_2d_1V_m$ represents the stoke work $SW \approx P_m\ SV$, where $SV \approx (V_{ed} - V_m)$ is the stroke volume. The area $d_3d_2d_1$ = CW apparently corresponds to

the energy absorbed by the passive medium of the myocardium. The area $d_1V_mV_{om}$ = PE apparently corresponds to the energy related to the internal metabolism of the myocardium. Point d_5 is the middle point of the segment d_3V_{om} with abscissa $V_{mid} = 0.5 (V_{ed} + V_{om})$., at which point the area CW_{mid} = TW/4 and the stroke work SW reaches its maximum value SW_{max}. The area SWRe = CW - CW_{mid} is not to be confused with the stroke work reserve SWR = SW_{max} - SW, SWR is the amount of energy that can be supplied to the systemic circulation before reaching the maximum value SW_{max} when the point d_1 coincides with the midpoint d_5 in figure 1. From figure 2, we see that when d_1 coincides with d_5 in figure 1, SWR = SWRe = 0 and CW = PE as verified by using the experimental clinical data published by Asanoi., *et al*. [29].

Figure 1: Simplified drawing of the PVR in the left ventricle. During a normal ejecting contraction, the rectangle Vedd2d1Vm represents the PV-loop (enclosing the stroke work SW). The left ventricular pressure Pm is assumed constant during the ejection phase for simplicity. It is assumed that Pm ≈ Pes the end-systolic pressure, Vm ≈ Ves the end-systolic volume. CW = triangular area d1d2d3, PE = triangular area d1VmVom, TW = CW + SW + PE is the total area under the ESPVR. The ESPVR is represented by the segment of line d3Vom with slope Emax, and midpoint d5 with volume Vmid; the line with slope E is an intermediate position. Note the change △Piso and △Pisom corresponding the change △Ved in the end-diastolic volume according to the Frank-Starling mechanism.

Figure 2: Relations between the ratio of areas CW/TW, PE/TW, SWR/TW and SWRe/TW. Note that SWR = SWRe = 0 correspond to CW = PE. Data correspond to three clinical groups: (a) EF >= 60% '*'; (b) 40% <= EF <= 59% 'o'; (c) EF <= 39% 'x'. Experimental data from Asanoi., *et al*. [29].

The ventricular elastance $E_{max} = P_m/(V_m - V_{om})$ and the vascular elastance $e_{am} = P_m/SV$ are related by the following relations

$E_{max}/e_{am} = SV/(V_m - V_{om})$ ------(7a)

$E_{max}/e_{am} = (P_{isom} - P_m)/P_m$ ------(7b)

$E_{max}/e_{am} = 2*CW/SW$ ----------(7c)

The three relations show the complex interrelation between the parameters controlling the left ventricular contraction. From the similarity of the triangles $d_3d_2d_1$ and $d_3V_{ed}V_{om}$ one can derive the important relation

$SV/(V_{ed} - V_{om}) = (P_{isom} - P_m)/P_{isom}$ ----------(8)

One can immediately notice that the EF = SV/V_{ed} is an approximation to $SV/(V_{ed} - V_{om})$ when we put V_{om} = 0, which evidently implies an approximation in P_{isom} as shown in figure 5. From the preceding relations one can derive

$(V_{ed} - V_{om})/(V_m - V_{om}) = P_{isom}/P_m$ --------(9)

The preceding equations show some relations between the parameters describing the ventricular cavity and the pressures

acting on the myocardium, this link is important in order to fully understand the connection between the state of the left ventricle and the state of the myocardium that is basic for the understanding the mechanics of cardiac contraction.

EF and Pisom

Some experimental applications of the preceding results are presented in the following. Figure 3 shows cases with EF = SV/V_{ed} around the horizontal line EF ≈ 0.63 (right side) (0.59 < EF < 0.65) that are considered as normal in the clinical practice, the corresponding values of CW/SW (Equ. (7c)) are presented by a broken line on the left side of figure 3 with 0.65 < CW/SW < 2.6 (normal values of $(P_{isom} - P_m)/P_m \approx 2$ corresponds to $E_{max}/e_{am} \approx 2$ and CW/SW ≈ 1 as will be explained later on in section 6.

Figure 3: (left side) Variation of CW/SW = 0.5*(Pisom - Pm)/Pm = 0.5*SV/(Vm - Vom) = 0.5*Emax/eam with Vom/Vm. (right side) Variation of EF = SV/Ved with Vom/Vm. Explanation as in text. Data correspond to three clinical groups: (a) EF >= 60% '*'; (b) 40% <= EF <= 59% 'o'; (c) EF <= 39% 'x'. Experimental data from Asanoi., *et al*. [29].

The division of the abscissa by V_m in figure 3 is to avoid normalisation with respect to body surface as in the data of Asanoi., *et al*. [29]. Equation (9) is represented in figure 4. If we neglect V_{om} in the calculation of the ratio $(V_{ed} - V_{om})/(V_m - V_{om})$, we get $V_{ed}/V_m = 1/(1 - EF)$ and for EF ≈ 0.63, we get $V_{ed}/V_m \approx 2.7$ as shown by the horizontal line in figure 5 (right side). These values are considered as normal in the clinical practice, the corresponding values of P_{isom}/P_m are represented by a broken line on the left side of figure 4 with $2.3 < P_{isom}/P_m < 6.2$ (normal value of $P_{isom}/P_m \approx 3$ corresponds to $E_{max}/e_{am} \approx 2$).

Figure 4: (left side) Variation of Pisom/Pm = (Ved - Vom)/(Vm - Vom) with Vom/Vm. (right side) Variation of Ved/Vm with Vom/Vm. Explanation as in text. Data correspond to three clinical groups: (a) EF >= 60% '*'; (b) 40% <= EF <= 59% 'o'; (c) EF <= 39% 'x'. Experimental data from Asanoi., *et al*. [29].

The preceding results show the difficulty of neglecting V_{om} in the calculation of the indexes used for classification of clinical data. This is further illustrated in figure 5, in which it is shown that neglecting V_{om} in the calculation amounts to replacing the gradient of pressures $(P_{isom} - P_m)/P_{isom}$ by a gradient $(P'_{isom} - P_m)/P'_{isom}$ (see Equ. (8)) in which the peak isovolumic pressure P'_{isom} is different from the actual value P_{isom}. Also the ESPVR represented by the line d_3V_{om} is replaced by the line d'_3O with $V_{om} = 0$ (upper and lower graphics in Figure 5). Areas under the ESPVR are also affected, but the ejection fraction $EF = (V_{ed} - V_m)/V_{ed}$ is the same for the lines d'_3O and d_3V_{om}. Note also that the abscissa $V_{mid} = 0.5*(V_{ed} + V_{om})$ of the midpoint d_5 is such that $V_{mid} > 0.5*V_{ed}$ when $V_{om} > 0$ (upper graphics in Figure 5), and $V_{mid} < 0.5*V_{ed}$ when $V_{om} < 0$ (lower graphics in Figure 5), these results are shown in figure 6 (left side). Similarly for the ejection fraction at the midpoint d_5, $EF_{mid} = (V_{ed} - V_{mid})/V_{ed} = 0.5*(1 - V_{om}/V_{ed})$. We have $EF_{mid} < 0.5$ for $V_{om} > 0$, and $EF_{mid} > 0.5$ for $V_{om} < 0$, these results are shown in figure 6 (right side). Figure 6 shows $V_{mid} \approx 0.5\ V_{ed}$ only for $V_{om} \approx 0$ (left side), and that $EF_{mid} \approx 0.5$

only for $V_{om} \approx 0$ (right side), otherwise the relations $V_{mid} \approx 0.5*(V_{ed} + V_{om})$ and $EF_{mid} \approx 0.5*(1 - V_{om}/V_{ed})$ should apply at the midpoint d_5 that show the evident dependence on V_{om}.

In order to show that the mathematical formalism is consistent with more than one set of clinical data, we have applied some relations to clinical data taken from Asanoi., *et al*. [29], and from Mehmel., *et al*. [7]. In figure 7a and figure 7b (left side), it is verified that $V_{mid}/V_m = 1$ for $E_{max}/e_{am} = 1$ (d_1 coincides with midpoint d_5 in figure 1). In figure 7a (right side) we see that for the normal value of $E_{max}/e_{am} = 2$, the EF varies approximately from 0.54 to 0.72, in figure 7b (right side) we see that for the normal value of $E_{max}/e_{am} = 2$, the EF varies approximately from 0.54 to 0.66. It is further shown in figure 8a and figure 8b (left side) EF - $EF_{mid} = 0$ corresponds to $V_{mid}/V_m = 1$ (d_1 coincides with midpoint d_5 in figure 1). In figure 8a (right side) we see the variation of $EF_{mid} = 0.5*(1 - V_{om}/V_{ed})$ with V_{om} from approximately 0.33 to approximately 0.54 at $V_{mid}/V_m \approx 1$ (when d_1 coincides with midpoint d_5), and a similar relation in figure 8b (right side) with EF_{mid} varying from 0.46 to 0.56. This variation in the value of EF_{mid} at $V_{mid}/V_m \approx 1$ reflects the dependence on V_{om}. Note that $V_{mid}/V_m < 1$ corresponds to d_1 above the midpoint d_5 on the ESPVR as explained in connection with figure 1 and it corresponds to a depressed state of the myocardium.

Figure 6: (left side) Graphics indicates that Vmid > 0.5*Ved for Vom > 0, and Vmid < 0.5*Ved for Vom < 0, Vmid = 0.5*Ved only for Vom = 0. (right side) Graphics indicates that EFmid < 0.5 for Vom > 0, and EFmid > 0.5 for Vom < 0, EFmid = 0.5 only for Vom = 0. Data correspond to three clinical groups: (a) EF >= 60% '*'; (b) 40% <= EF <= 59% 'o'; (c) EF <= 39% 'x'. Experimental data from Asanoi., *et al*. [29].

Figure 5: Approximation Vom = 0 that leaves the ejection fraction EF = (Ved - Vm)/Ved unchanged. The actual ESPVR d3Vom is approximated by d'3O, and the peak isovolumic pressure Pisom is replaced by P'isom.

Figure 7a: (left side) shows that Vmid/Vm = 1 when Emax/eam = 1 (d1 and d5 coincides in Figure 1). (right side) For the normal value of Emax/eam = 2, the EF varies approximately from 0.54 to 0.66. Cases of HFrEF correspond to Emax/eam <= 1 and are indicated 'x'. Data correspond to three clinical groups: (a) EF >= 60% '*'; (b) 40% <= EF <= 59% 'o'; (c) EF <= 39% 'x'. Experimental data from Asanoi., *et al*. [29].

Figure 7b: (left side) shows that Vmid/Vm = 1 when Emax/eam = 1 (d1 and d5 coincides in Figure 1). (right side) For the normal value of Emax/eam ≈ 2, the EF varies approximately from 0.54 to 0.66. Data correspond to three groups: (a) control '*'; (b) after oral isosorbide-dinitrate 'o'; (c) during infusion of methoxamine 'x'. Experimental data from Mehmel., *et al*. [7].

Figure 8a: (left side) EF - EFmid = 0 corresponds to Vmid/Vm = 1. (right side) Variation of EFmid = 0.5*(1 - Vom/Ved) with Vom at Ved/Vm = 1. Explanation as in text. Data correspond to three clinical groups: (a) EF >= 60% '*'; (b) 40% <= EF <= 59% 'o'; (c) EF <= 39% 'x'. Experimental data from Asanoi., *et al*. [29].

Figure 8b: (left side) EF - EFmid = 0 corresponds to Vmid/Vm = 1. (right side) Variation of EFmid = 0.5*(1 - Vom/Ved) with Vom for Ved/Vm ≈ 1. Explanation as in text. Data correspond to three groups: (a) control '*'; (b) after oral isosorbide-dinitrate 'o'; (c) during infusion of methoxamine 'x'. Experimental data from Mehmel., *et al*. [7].

Figure 9 shows the difference between the correct values $SV/(V_{ed} - V_{om}) = (P_{isom} - P_m)/P_{isom}$ or $SV/(V_m - V_{om}) = (P_{siom} - P_m)/P_m$, and the approximate values $SV/V_{ed} = (P'_{isom} - P_m)/P'_{isom}$ or $SV/V_m = (P'_{isom} - P_m)/P_m$ when $V_{om} = 0$, P'_{isom} as shown in figure 5.

Figure 9a: (left side) Relation between SV/(Ved - Vom) - SV/Ved and SV/(Vm - Vom) - SV/Vm. (right side) Relation between SV/(Ved - Vom) - SV/Ved and Vom/Vm. Data correspond to three clinical groups: (a) EF >= 60% '*'; (b) 40% <= EF <= 59% 'o'; (c) EF <= 39% 'x'. Experimental data from Asanoi., *et al*. [29].

Figure 9b: (left side) Relation between SV/(Ved - Vom) - SV/Ved and SV/(Vm - Vom) - SV/Vm. (right side) Relation between SV/(Ved - Vom) - SV/Ved and Vom/Vm. Data correspond to three groups: (a) control '*'; (b) after oral isosorbide-dinitrate 'o'; (c) during infusion of methoxamine 'x'. Experimental data from Mehmel., *et al*. [7].

Classification of the state of the myocardium

When the point d_1 on the segment d_3V_{om} in figure 1 moves upward, the stroke work SW will reach its maximum value SW_{max} when d_1 coincides with the midpoint d_5 with abscissa $V_{mid} = 0.5*(V_{ed} + V_{om})$, stroke volume $SV_{mid} = 0.5*(V_{ed} - V_{om})$ and ejection fraction $EF_{mid} = SV_{mid}/V_{ed} = 0.5*(1 - V_{om}/V_{ed})$. Beyond d_5, a move of d_1 upward results in a reduction in SW. The position of the point d_1 with respect to the midpoint d_5 as expressed by the ratio $E_{max/}e_{am} = SV/(V_m - V_{om})$ is used for a possible classification of the state of the myocardium into three groups as follows:

- The values $E_{max}/e_{am} \approx 2$ with $P_{isom}/P_m \approx 3$ and $SW < SW_{max}$ correspond to a normal physiological state of the myocardium, with d_1 below d_5 on the ESPVR. It is shown in the Appendix that this state corresponds to maximum efficiency of the myocardium for oxygen consumption, as explained in [30,31]. In this case we have at point d_1 $EF > EF_{mid}$ or $SV/V_{ed} > 0.5*(1 - V_{om}/V_{ed})$. An increase in afterload represented by P_m results in an increase in SW as it should, with possible changes in E_{max} and V_{om}, but always in a way to maintain $SW < SW_{max}$.
- The values $E_{max}/e_{am} \approx 1$ with $P_{isom}/P_m \approx 2$ and $SW \approx SW_{max}$ correspond to a mildly depressed state of myocardium. In this case d_1 coincides with the midpoint d_5 (or is just below) on the ESPVR. We have $EF \approx EF_{mid}$ or $SV/V_{ed} \approx 0.5*(1 - V_{om}/V_{ed})$. An increase in afterload P_m results in a decrease in SW (d_1 moves above d_5 on the ESPVR), causing cardiac insufficiency.
- The values $E_{max}/e_{am} < 1$ with $P_{isom}/P_m < 2$ and $SW < SW_{max}$ correspond to a severely depressed state of the myocardium. In this case d_1 is above the midpoint d_5 on the ESPVR. We have $EF < EF_{mid}$ or $SV/V_{ed} < 0.5*(1 - V_{om}/V_{ed})$. An increase in afterload P_m results in a further decrease in SW when an increase is expected, causing severe cardiac insufficiency.

Experimental verification of these results for the left ventricle in the case of experiments carried out on dogs has been reported by Burkhoff and Sagawa [32], the extension of these results to the left ventricle in the case of experiments carried out on patients has been reported by Asanoi., *et al*. [29], and the extension of these results to the right ventricle in the case of experiments carried out on dogs has been reported by Brimioulle., *et al*. [28].

One can expect that during adaptation to load variation represented by a change in P_m, the parameters V_{om}, E_{max} and P_{isom} can change in a way to maintain a stroke work reserve $SWR = SW_{max} - SW > 0$, until a limit is reached beyond which this process of adaptation fails. Heart failure as defined in this study happens when an increase in load demand represented by an increase in P_m results in a reduction of stroke work SW creating cardiac insufficiency. This definition of HF is not unique, it is clear the HF can be caused by other pathologies.

The graphics in figure 10 illustrates again the importance of the ESPVR in the interpretation of the EF, the figure shows two cases HFnEF ($EF < EF'_{mid}$, $EF'_{mid} = 0.5*(1 - V'_{om}/V_{ed})$), one is a case of reduced contractility (d_1 above midpoint d'_5 on the dotted line, upper graphics) and the other is a case of hypertension (d'_1 above midpoint d'_5 on the dotted line, lower graphics). Both have the same $EF = SV/V_{ed}$ of a normal state with d_1 below midpoint d_5 on the solid ($EF > EF_{mid}$, $EF_{mid} = 0.5*(1 - V_{om}/V_{ed})$). Note that EF decreases as d_1 moves upwards on the ESPVR. Note also that that V_{om} can be negative, meaning that an abnormal state with $EF < EF_{mid}$, $EF_{mid} = 0.5*(1 + |V_{om}|/V_{ed})$ can still have an $EF > 0.5$ suggesting a HFpEF or a HFnEF.

Figure 10: Simplified graphics showing the importance of the ESPVR in understanding the EF = SV/Ved. (lower graphics): Normal case with d_1 below midpoint d_5 on the ESPVR (solid line); hypertension with d'1 above midpoint d'_5 on the ESPVR (dotted line). (upper graphics): Normal case with d_1 below mid-point d_5 on the ESPVR (solid line); reduced contractility with d_1 above midpoint d'_5 on the ESPVR (dotted line). Note that the normal clinical case and two abnormal clinical cases have the same EF = SV/Ved.

Figure 11: (left side) Correct curve with SV/(Ved - Vom) = 0.5 for Emax/eam = 1, and SV/(Ved - Vom) = 2/3 for Emax/eam = 2. (right side) Approximate curve by putting Vom = 0, points indicated ? with SV/Ved ≈ 0.54 are a possible example of HFpEF. Explanation as in text. Data correspond to three clinical groups: (a) EF >= 60% '*'; (b) 40% <= EF <= 59% 'o'; (c) EF <= 39% 'x'. Experimental data from Asanoi., *et al*. [29].

A possible definition of HFpEF can correspond to group (b) mentioned above, with d_1 with coordinates (V_m, P_m) slightly below the midpoint d_5 (V_{mid}, $P_{isom}/2$) on the ESPVR (V_m <= V_{mid}, EF >= EF_{mid}), but with d_1 moving at d_5 or above d_5 (V_m >= V_{mid}, EF <= EF_{mid}) as a result of an increase in afterload P_m. Figure 11 (right side) illustrates some cases of HFpEF with a group of data marked ? with EF = SV/V_{ed} ≈ 0.54, but with E_{max}/e_{am} ≈ 1 (d_1 nearly coincident with d_5), figure 11 (left side) shows the correct curve with $SV/(V_{ed} - V_{om})$ = 0.5 at E_{max}/e_{am} = 1. The case HFrEF can correspond to group (c) mentioned above with EF < EF_{mid} and $V_m > V_{mid}$ (or $V_{mid}/V_m < 1$) as illustrated in figure 7a (right side) for the data indicated 'x' with E_{max}/e_{am} <= 1.

Percentage occurrence of HF

The experimental data (round circles) in figure 12a (left side) and figure 12b (left side) are taken from the thesis of da Mota [33], they represent the percentage occurrence of HF plotted against the left ventricular ejection fraction LVEF = EF*100. A least squares fit of these data was calculated and the curve obtained was used to interpolate the data taken from Asanoi., *et al*. [29] and Mehmel., *et al*. [7], the results are respectively shown in figure 12a (right side) and Figure 12b (right side). Figures 12a and 12b show a minimum of these curves around EF = SV/V_{ed} ≈ 0.63 to 0.65, which corresponds approximately to $SV/(V_{ed} - V_{om}) = (P_{isom} - P_m)/P_{isom}$ ≈ 2/3 (corresponding to E_{max}/e_{am} ≈ 2). Figure 12a (right side) show how the EF can be used to relate the state of the myocardium to the probability of occurrence of HF and can be efficiently implemented in routine clinical work.

Areas under ESPVR

The areas under the ESPVR have units of energy and are sensitive indexes to reflect the state of the myocardium. As mentioned in connection with figure 1 and figure 2, the area $SWRe = CW - CW_{mid}$ is not to be confused with the stroke work reserve $SWR = SW_{max} - SW$, SWR is the amount of energy that can be supplied to the systemic circulation before reaching the maximum value SW_{max} when the

point d_1 coincides with the midpoint d_5 in figure 1. Figures 13a and 13b show the variations of SWR/SW with $SV/(V_{ed} - V_{om}) = (P_{isom} - P_m)/P_{isom}$ (left side), and the variation of SWRe/SW with $SV/(V_{ed} - V_{om}) = (P_{isom} - P_m)/P_{isom}$. Like with other results, the comparison of the results obtained by using the data taken from Asanoi., *et al*. [29] and the data taken from Mehmel., *et al*. [7] show the consistency of the mathematical formalism used.

Figure 12a: Experimental data show a relation between occurrence of HF (%) and LVEF = EF*100. Red line indicates calculated least squares fit, experimental data taken from da Mota [33]. (right side) Relation between interpolated data of occurrence of HF (%) obtained for the experimental data of LVEF = EF*100 obtained from Asanoi., *et al*. [29]. Data correspond to three clinical groups: (a) EF >= 60% '*'; (b) 40% <= EF <= 59% 'o'; (c) EF <= 39% 'x'.

Figure 13a: (left side) Variation of SWR/SW with SV/(Ved - Vom) = (Pisom - Pm)/Pisom. (right side) Variation of SWRe/SW with SV/(Ved - Vom) = (Pisom - Pm)/Pisom. Explanation as in text. Data taken from Asanoi., *et al*. [29] correspond to three clinical groups: (a) EF >= 60% '*'; (b) 40% <= EF <= 59% 'o'; (c) EF <= 39% 'x'.

Figure 12b: (left side) Experimental data show a relation between occurrence of HF (%) and LVEF = EF*100. Red line indicates calculated least squares fit, experimental data taken from da Mota [33]. (right side) Relation between interpolated data of occurrence of HF (%) obtained for the experimental data of LVEF = EF*100 taken from Mehmel., *et al*. [7]. Data on the right side correspond to three groups: (a) control '*'; (b) after oral isosorbide-dinitrate 'o'; (c) during infusion of methoxamine 'x'.

Figure 13b: (left side) Variation of SWR/SW with SV/(Ved - Vom) = (Pisom - Pm)/Pisom. (right side) Variation of SWRe/SW with SV/(Ved - Vom) = (Pisom - Pm)/Pisom. Explanation as in text. Data taken from Mehmel., et al. [7] correspond to three groups: (a) control '*'; (b) after oral isosorbide-dinitrate 'o'; (c) during infusion of methoxamine 'x'.

Although the trend has been to try to link the oxygen consumption VO_2 with the area PVA = PE + SW [34] under the ESPVR, the inclusion of P_{isom} in the mathematical formalism describing the ESPVR suggests that the total area under the ESPVR can be used in studying the energy balance of the myocardium as previously discussed by the author [30,31]. For this purpose we note that we have the following relations between the areas

$$PE = 0.5*P_m*(V_m - V_{om}) = 0.5*(e_{am}/E_{max})*SW \text{ ----(10)}$$

$$CW = 0.5*(P_{isom} - P_m)*SV = 0.5*(E_{max}/e_{am})*SW\text{---------- (11)}$$

$$PE*CW = 0.25*SW^2\text{ ---------- (12)}$$

By writing $x = (CW/TW)^{1/2}$ and $y = (PE/TW)^{1/2}$, we can verify that we have 2*x*y = SW/TW. We also have

$$(x+y)^2 = x^2 + y^2 + 2*x*y = (CW/TW) + (PE/TW) + (SW/TW) = 1\text{--------- (13)}$$

From which we can deduce that x + y = 1, easily verified from the following equations

$$x = (E_{max}/e_{am})/(1 + E_{max}/e_{am}) = (CW/TW)^{1/2}\text{ ------(14)}$$

$$y = 1/(1 + E_{max}/e_{am}) = (PE/TW)^{1/2}\text{ ---------(15)}$$

These two last relations are shown in Figure 14 for the data taken from Mehmel., *et al*. [7], a similar relation can be calculated for the data taken from Asanoi., *et al*. [29].

We now turn to the calculation of the energy consumed in one cycle by the myocardium that we express in the form

$$E_1 = k_p\ PE/TW + k_s\ SW/TW + k_c\ CW/TW\text{ ----------(16)}$$

We suppose that there is an optimization process that is taking place for an optimal use of VO_2 by the myocardium. How this optimization process can be carried out in order to calculate $E_{max}/e_{am} = x/(1 - x)$ is given in the Appendix, in which it is shown that by taking into consideration the constraint that 1 = PE/TW + SW/TW+ CW/TW, we can carry out the optimization process by using the formula

$$E_2 = k_p + (k_s - k_p)\ SW/TW + (k_c - k_p)\ CW/TW\text{ ------(17a)}$$

$$E_2 = k_p + (k_s - k_p)\ 2xy + (k_c - k_p)\ x^2\text{ ---------(17b)}$$

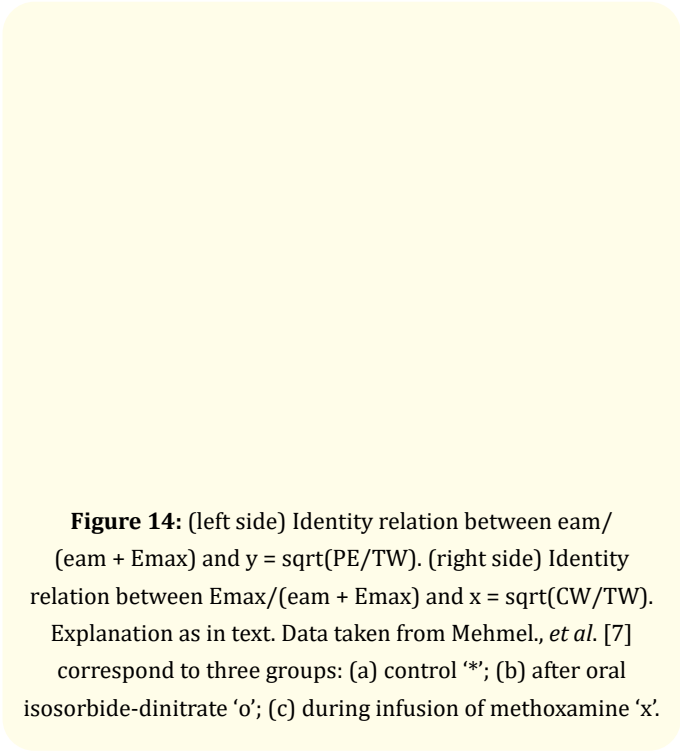

Figure 14: (left side) Identity relation between eam/(eam + Emax) and y = sqrt(PE/TW). (right side) Identity relation between Emax/(eam + Emax) and x = sqrt(CW/TW). Explanation as in text. Data taken from Mehmel., *et al*. [7] correspond to three groups: (a) control '*'; (b) after oral isosorbide-dinitrate 'o'; (c) during infusion of methoxamine 'x'.

By taking into account that y = (1 - x) and calculating the derivative $dE_2/dx = 0$, we get

$$(k_s - k_p)/(k_s - k_c) = x/(1 - x) = E_{max}/e_{am}\text{ ----------(18)}$$

From which we deduce the following results:

$k_p = 1, k_s = 4, k_c = 3, E_{max}/e_{am} = 3, E_2 = 3\ SW/TW + 2\ CW/TW + 1$ --------(19a)

$k_p = 1, k_s = 3, k_c = 2, E_{max}/e_{am} = 2, E_2 = 2\ SW/TW + CW/TW + 1$ ----------(19b)

$k_p = 1, k_s = 7, k_c = 4\ E_{max}/e_{am} = 2; E_2 = 6\ SW/TW + 3\ CW/TW + 1$ ----------(19c)

$k_p = 1, k_s = 2, k_c = 1, E_{max}/e_{am} = 1, E_2 = SW/TW + 1$ ----------(19d)

$k_p = 1, k_s = 2, k_c = 0, E_{max}/e_{am} = 1/2, E_2 = SW/TW - CW/TW + 1$ ----------(19e)

Equations (19b) and (19d) are shown in figure 15a and 15b, in one case the maximum of the curve appears at $E_{max}/e_{am} = 1$ (Equs. (19d)), in the other case the maximum of the curve appears at

E_{max}/e_{am} = 2 (Equs. (19b)). Equations (19a) and (19e) are shown in figure 16a and 16b, the respective maximum of each curve appears at E_{max}/e_{am} = 3 (left side) and at E_{max}/e_{am} = 1/2 (right side), note that E_{max}/e_{am} = 1/2 corresponds to point d_1 above the midpoint d_5 on the ESPVR (see Figure 1). Note also that the coefficients k_p, k_s, and k_c are not static and may vary from cycle to cycle depending for instance on change in contractility, in preload or afterload as a result of an adaptation process to load condition by the myocardium.

Figure 15a: (left side) The curve SW/TW + 1 has its maximum at Emax/eam = 1. (right side) The curve 2*SW/TW + CW/TW + 1 has its maximum at Emax/eam = 2. Explanation as in text. Data taken from Asanoi., *et al*. [29] correspond to three clinical groups: (a) EF >= 60% '*'; (b) 40% <= EF <= 59% 'o'; (c) EF <= 39% 'x'.

Figure 15b: (left side) The curve SW/TW + 1 has its maximum at Emax/eam = 1. (right side) The curve 2*SW/TW + CW/TW + 1 has its maximum at Emax/eam = 2. Explanation as in text. Data taken from Mehmel., *et al*. [7] correspond to three groups: (a) control '*'; (b) after oral isosorbide-dinitrate 'o'; (c) during infusion of methoxamine 'x'.

The case E_{max}/e_{am} = 2 correspond also to the case of maximum efficiency defined as operation in a way to maximize the energy delivered to the systemic circulation in each cycle. This is expressed in Equ. (20) that tends to maximize the numerator and to minimize the denominator.

Figure 16a: (left side) The curve 3*SW/TW + 2*CW/TW + 1 has its maximum at Emax/eam = 3. (right side) The curve SW/TW - CW/TW + 1 has its maximum at Emax/eam = 0.5. Explanation as in text. Data taken from Asanoi., *et al*. [29] correspond to three clinical groups: (a) EF >= 60% '*'; (b) 40% <= EF <= 59% 'o'; (c) EF <= 39% 'x'.

Figure 16b: (left side) The curve 3*SW/TW + 2*CW/TW + 1 has its maximum at Emax/eam = 3. (right side) The curve SW/TW - CW/TW + 1 has its maximum at Emax/eam = 0.5. Explanation as in text. Data taken from Mehmel., *et al*. [7] correspond to three groups: (a) control '*'; (b) after oral isosorbide-dinitrate 'o'; (c) during infusion of methoxamine 'x'.

$\eta_1 = (\alpha_1 PE + \alpha_2 SW + \alpha_3 CW)/(\alpha_1 PE + \alpha_3 CW)$ --------(20)

Which is also equivalent to seeking the maximum of

$\eta_2 = SW/(\alpha_1 PE + \alpha_3 CW)$ -------(21)

The solution is discussed in the Appendix by calculating the derivative $d\eta_2/dx = 0$. One obtains

$x^2/(1 - x)^2 = \alpha_1/\alpha_3 = (E_{max}/e_{am})^2$ ---(22)

By substituting $\alpha_1/\alpha_3 = 4$ in Equ. (21) (as discussed in [30,31]), we get figure 17 (left side) that shows the case of maximum efficiency SW/(4*PE + CW) plotted against E_{max}/e_{am}, with a maximum at $E_{max}/e_{am} = 2$. Figure 17 (right side) shows the case SW/(PE + CW) plotted against E_{max}/e_{am} with a maximum at $E_{max}/e_{am} = 1$ as discussed in the Appendix.

Figure 17: (left side) The curve SW/(4*PE + CW) has its maximum at Emax/eam = 2. (right side) The curve SW/(PE + CW) has its maximum at Emax/eam = 1. Calculation is based on the assumption of maximum efficiency. Explanation as in text. Data taken from Asanoi., *et al*. [29] correspond to three clinical groups: (a) EF >= 60% '*'; (b) 40% <= EF <= 59% 'o'; (c) EF <= 39% 'x'.

Discussion

The maximum active pressure generated by the myocardium during the systolic phase (also called peak isovolumic pressure P_{isom} by physiologists) is mainly determined in the diastolic phase by the internal metabolism of the myocardium and the initial stretch of the cardiac muscle measured at end-diastole according to the Frank-Starling mechanism, as shown in figure 1. The introduction of P_{isom} in the formalism describing the ESPVR has revealed interesting relations between the EF and the parameters describing the ESPVR, in particular $EF = SV/V_{ed} = (P'_{isom} - P_m)/P'_{isom}$ appears as an approximation to $SV/(V_{ed} - V_{om}) = (P_{isom} - P_m)/P_{isom}$ as shown in figure 5.

The link between volume parameters of the left ventricle and pressure parameters of the myocardium is given by the slope E_{max} and the intercept V_{om} of the ESPVR with the volume axis. In particular it is explained in this study that the ratio E_{max}/e_{am} can be used to classify the state of the myocardium into normal, mildly depressed or severely depressed state, and that V_{om} can be used in the definition of HFnEF and HFpEF ($EF < EF_{mid}$, $EF_{mid} = 0.5*(1 - V_{om}/V_{ed})$). In figure 7a (right side) it is shown that HFrEF can be defined as EF <= 0.39, which corresponds to $E_{max}/e_{am} <= 1$. Bivariate analysis of data is superior to univariate analysis of data, and this is evident from the relation between EF of the percentage occurrence of HF shown in figure 12a and 12b, the curves shown in the two figures can efficiently be implemented for routine clinical work.

Some examples have been given on the way the areas under the ESPVR can be used to measure the energetic performance of the myocardium. It should be clear that the ESPVR is not a static relation, from cycle to cycle changes may happen in the end-systolic parameters describing the ESPVR, for instance as a result of change in contractility of the cardiac muscle, or as a result of adaptation to preload or afterload condition. One can suppose that this adaptation to load condition is conducted in a way to ensure optimal efficiency of the heart as a pump. This is what is discussed in the Appendix where models for the optimal performance of the myocardium are presented based on a study of the areas under the ESPVR. The results are shown in figure 15a to 17.

An important problem not discussed in this study is the accurate non-invasive calculation of E_{max} and V_{om}, some preliminary ideas can be found in [12,35].

Conclusion

In this study mathematical results are presented that add to our understanding of the mechanics of cardiac contraction. Applications to clinical data published in the literature can be

considered as a confirmation of the consistency of the mathematical formalism used. Generally bivariate (or multivariate) analysis of data for the purpose of classification of clinical data are superior to univariate analysis of data (by using one index like EF). No one index gives perfect segregation between all clinical cases, some indexes are better than others depending on the clinical cases under consideration.

Appendix

Methods of optimization of the areas under the ESPVR

We would like to optimize the distribution of the areas PE, SW, CW under the ESPVR in a way to maximize

$$E_1 = k_p (PE/TW) + k_s (SW/TW) + k_c (CW/TW) \text{ ----------(A1)}$$

By using the notation of Equs (16) and (17), Equ. (A1) can be written in the form

$$E_1 = k_p y^2 + 2 k_s xy + k_c x^2 \text{ ----------(A2)}$$

$$E_1 = k_p (1 - x)^2 + 2 k_s x (1 - x) + k_c x^2 \text{ ----------(A3)}$$

The necessary condition for a maximum of E_1 is that the derivative $dE_1/dx = 0$, which gives

$$(k_s - k_p)/(k_s - k_c) = x/(1 - x) = E_{max/}e_{am} \text{ ----------(A4)}$$

This is Equ. (18) in the main text.

Finally we come to the maximum efficiency of the left ventricle, defined as maximizing the energy delivered to the systemic circulation compared to the total energy consumed in one cycle of the heart. For this purpose we consider the following expression given in Equ. (20)

$$\eta_1 = (\alpha_1 PE + \alpha_2 SW + \alpha_3 CW)/(\alpha_1 PE + \alpha_3 CW) \text{ ----------(A5)}$$

It is chosen in a way to maximize the numerator and to minimize the denominator in order to have a maximum for η_1, it is also equivalent to seeking the maximum of

$$\eta_2 = SW/(\alpha_1 PE + \alpha_3 CW) \text{----------} (A6)$$

By using the x and y = 1 - x notation, Equ. (A6) takes the form

$$\eta_2 = (2 x y)/(\alpha_1 y^2 + \alpha_3 x^2) \text{ ----------(A7)}$$

By calculating $d\eta_2/dx = 0$, we get

$$\alpha_1/\alpha_3 = x^2/(1 - x)^2 = (E_{max}/e_{am})^2 \text{ ---------(A8)}$$

From references [30,31] it was observed that maximum efficiency corresponds to $\alpha_1/\alpha_3 \approx 4$, which gives $E_{max}/e_{am} \approx 2$. Figure 17 (left side) shows the case of maximum efficiency SW/(4*PE + CW) plotted against E_{max}/e_{am}, with a maximum at $E_{max}/e_{am} = 2$. The curve $SW/((\alpha_1/\alpha_3) *PE + CW)$ has a maximum at $(\alpha_1/\alpha_3)^{1/2}$ that varies with this ratio, figure 17 (right side) shows the case SW/(PE + CW) plotted against E_{max}/e_{am} with a maximum at $E_{max}/e_{am} = 1$. It should be clear that the curve of maximum efficiency is not a static curve, it may vary from cycle to cycle with the variation in the ratio α_1/α_3, for instance as a result of variation in contractility or load condition.

Bibliography

1. Frank O. "Die Grundform des arteriellen Pulses". *Zeit für Biol* 37 (1899): 483-526.

2. Kuhtz-Buschbeck JP., *et al*. "Rediscovery of Otto Frank's contribution to science". *Journal of Molecular and Cellular Cardiology* 119 (2018): 96-103.

3. Kjorstad KE., *et al*. "Pressure-volume based single-beat estimation cannot predict left ventricular contractility in vivo". *American Journal of Physiology* 282 (2002): H1739-H1750.

4. Burkhoff D., *et al*. "Assessment of systolic and diastolic ventricular properties via pressure-volume analysis: A guide for clinical, translational, and basic researchers". *American Journal of Physiology* 289 (2005): H501-H512.

5. Suga H., *et al*. "Mechanical efficiency of the left ventricle as a function of preload, afterload, and contractility". *Heart and Vessels* 1 (1985): 3-8.

6. Carabello BA. "The role of end-systolic pressure-volume analysis in clinical assessment of ventricular function". *Trends in Cardiovascular Medicine* 1 (1991): 337-341.

7. Mehmel HC., *et al*. "The linearity of the end-systolic pressure-volume relationship in man and its sensitivity for assessment of ventricular function". *Circulation* 63 (1981): 1216-1222.

8. Shoucri RM. "The pressure-volume relation and the mechanics of left ventricular contraction". *Japanese Heart Journal* 31 (1991): 713-729.

9. Shoucri RM. "Theoretical study of the pressure-volume relation in left ventricle". *American Journal of Physiology-Heart and Circulatory Physiology* 260 (1991): H282-H291.

10. Shoucri RM. "Mathematical aspects of the mechanics of left ventricular contraction". *International Journal of Design and Nature and Ecodynamics* 5.2 (2010): 173-188.

11. Shoucri RM. "Studying the mechanics of left ventricular contraction". *IEEE Engineering in Medicine and Biology Magazine* 17 (1998): 95-101.

12. Shoucri RM. "Ejection fraction and ESPVR, A study from a theoretical perspective". *International Heart Journal* 54 (2013): 318-327.

13. Shoucri RM. "Basic relations between ejection fraction and ESPVR". *Austin Journal of Clinical Cardiology* 1 (2014): 1-6.

14. Shoucri RM. "End-systolic pressure-volume relation, ejection fraction, and heart failure: Theoretical aspect and clinical applications". *Clinical Medicine Insights: Cardiology* 9 (2015): 1-10.

15. Shoucri RM. "Ejection fraction and ESPVR: A study in the mechanics of left ventricular contraction". *Cardiology Open Access (Austin)* 5.1 (2020): 37-47.

16. Shoucri RM. "Clinical applications of the areas under ESPVR: A review". in: Highlights on Medicine and Medical Research, vol. 10, chap. 2, editor: Dr John Yahya I. Elshimali (BP International) (2021): 10-15.

17. Shoucri RM. "A Basic Look at Ventricular Function and Cardiac Mechanics". in: Recent Development in Medicine and Medical Research, vol 4, chap. 5, editor: Naseem A. Qurashi (BP International) (2021): 31-45.

18. Kitzman DW., *et al*. "Exercise intolerance in patients with heart failure and preserved left ventricular systolic function: Failure of the Frank-Starling mechanism". *Journal of the American College of Cardiology* 17.5 (1991): 1065-1072.

19. Burkhoff D., *et al*. "Heart failure with a normal ejection fraction: Is it really a disorder of diastolic function?" *Circulation* 107 (2003): 656-658.

20. Sanderson JE. "Heart failure with a normal ejection fraction". *Heart* 93 (2007): 155-158.

21. Little WC. "Hypertension, heart failure, and ejection fraction". *Circulation* 118 (2008): 2223-2224.

22. Marwick TH. "Ejection fraction pros and cons". *Journal of the American College of Cardiology* 42.3 (2018): 736-742.

23. Naing P., *et al*. "Heart failure with preserved ejection fraction, a growing global epidemic". *Australian Journal of General Practice* 48 (2019): 465-471.

24. Sasayama S and Asanoi H. "Coupling between the heart and arterial system in heart failure". *The American Journal of Medicine* 90 (1991): 14-18.

25. Shoucri RM. "ESPVR, Ejection Fraction and Heart Failure". *Cardiovascular Engineering* 11 (2010): 207-212.

26. Maughan WL., *et al*. "Instantaneous pressure-volume relationship of the canine right ventricle". *Circulation Research* 44 (1979): 309-315.

27. Shoucri RM. "Pressure-volume relation in the right ventricle". *Journal of Biomedical Engineering* 15 (1993): 167-169.

28. Brimioulle S., *et al*. "Single-beat estimation of the right ventricular end-systolic pressure-volume relationship". *American Journal of Physiology-Heart and Circulatory Physiology* 284 (2003): 1625-1630.

29. Asanoi H., *et al*. "Ventriculo-arterial coupling in normal and failing heart in Humans". *Circulation Research* 65 (1989): 483-493.

30. Shoucri RM. "Possible clinical applications of the external work reserve of the myocardium". *Japanese Heart Journal* 35.6 (1994): 771-787.

31. Shoucri RM. "Theoretical study related to left ventricular energetics". *Japanese Heart Journal* 34.4 (1993): 403-417.

32. Burkhoff D and Sagawa K. "Ventricular efficiency predicted by an analytical model". *American Journal of Physiology* 250 (1986): R1021-R1027.

33. da Mota JPGF. "Intelligent modeling to predict ejection fraction from Echocardiographic reports". MSc thesis in Mechaniical Engineering, IST Técnico Lisboa, Portugal (2013).

34. Suga H. "Cardiac energetic: from Emax to pressure-volume area". *Clinical and Experimental Pharmacology and Physiology* 30 (2003): 580-585.

35. Shoucri RM. "Calculation of parameters of end-systolic pressure-volume relation in the ventricles". *Mathematical and Computer Modelling* 54 (2011): 1638-1643.

Assets from publication with us

- Prompt Acknowledgement after receiving the article
- Thorough Double blinded peer review
- Rapid Publication
- Issue of Publication Certificate
- High visibility of your Published work

Website: www.actascientific.com/

Submit Article: www.actascientific.com/submission.php

Email us: editor@actascientific.com

Contact us: +91 9182824667